

GUTPA/95/12/1
FSU-SCRI-95-121
OHSTPY-HEP-T-95-026
December 1995

The Heavy-Light Spectrum from Lattice NRQCD

A. Ali Khan ¹ and C. T. H. Davies ¹

University of Glasgow,
Glasgow G12 8QQ, UK

S. Collins ² and J. Sloan

Supercomputer Computations Research Institute
Florida State University
Tallahassee, FL 32306-4052, USA

J. Shigemitsu

The Ohio State University
Columbus, OH 43210, USA

Abstract

We present a lattice investigation of heavy-light mesons in the quenched approximation, using non-relativistic QCD for the heavy quark and a clover improved Wilson formulation for the light quark. A comprehensive calculation of the heavy-light spectrum has been performed for various heavy quark masses around the b . Our results for the $B_s - B_d$ splitting agree well with the experimental value. We find the $\Lambda_b - B$ splitting to be compatible with experiment, albeit with large error bars. Our $B^* - B$ splitting is slightly low, which could be explained as an effect of quenching. For the first time, we are able to estimate the mass of P states at the B and compare them with experiment.

PACS numbers: 12.38.Gc, 14.65.Fy, 14.40.Nd, 14.20.Mr

¹UKQCD Collaboration

²Present address: The University of Edinburgh, Edinburgh EH9 3JZ, U.K.

1 Introduction

Heavy-light hadrons containing a b quark are of topical interest in particle theory. Theoretical predictions for heavy-light meson decay constants are needed for an experimental determination of elements of the CKM matrix [1]. A theoretically interesting feature of heavy-light hadrons is that, in the limit of a very heavy quark mass m_Q , the dynamics simplify and can be described by an effective field theory (Heavy Quark Effective Theory) [2]. In the heavy quark limit $m_Q \rightarrow \infty$ additional symmetries between states of different spin and flavour appear which make it possible to relate different decay processes to each other and to make qualitative predictions about the spectrum. Away from the heavy quark limit a systematic expansion in the heavy quark mass can be performed whose coefficients have to be determined non-perturbatively. On the lattice this can be done from first principles.

Since, for the values of the lattice spacings which can be achieved in present computer simulations, the b quark mass is > 1 in lattice units, b quarks cannot be simulated directly using a naïve relativistic quark action. It has been suggested that heavy quarks around and above the charm can be simulated using a reformulation of a relativistic quark action [3], but there are indications that there are problems with this method in the b quark region [4], at least in the way the method has been implemented to date. So simulations are often done at smaller quark masses, up to the charm, and results extrapolated to the b . With this method it is very difficult to get certain spectral quantities, such as spin splittings, to agree with experiment. Simulations of heavy-light systems in the static (i.e. infinite mass) limit of the heavy quark give sensible results only for spectral quantities that are fairly independent of m_Q . For other quantities, contributions due to the finiteness of the heavy quark mass have to be calculated directly as perturbations in $1/m_Q$ (see e.g. [5]). In addition the signal-to-noise ratio is much worse than for propagating quarks.

The non-relativistic formulation of QCD (NRQCD) [6] however allows us, in principle, to simulate at the b quark mass. The largest momentum scale which governs discretization errors is not the heavy quark mass but the non-relativistic momentum of the heavy quark, which is much smaller. This method has been successful in precision spectroscopy of heavy-heavy systems such as Υ and J/Ψ mesons [7, 8]. In these systems the energy scale inside the meson is set by the kinetic energy of the heavy quarks, which is of the order of Λ_{QCD} . Relativistic corrections are included in a systematic expansion in v_Q^2 , where v_Q is the velocity of the heavy quark. For mesons with one heavy and one light quark the power counting rules for the non-relativistic expansion are determined by the fact that here the energy scale for the heavy quark inside the meson is the binding energy. For $m_Q \rightarrow \infty$ only the time derivative appears in the tree level Lagrangian. The covariant time derivative acting on the heavy quark spinor gives the quark

energy:

$$D_t Q \sim E_{\text{bind}} Q, \quad (1)$$

Due to momentum conservation the heavy and light quark momenta are equal in the rest frame of the meson:

$$m_Q v = p_Q = p_q \sim O(\Lambda_{QCD}), \quad (2)$$

where Λ_{QCD} takes a value around 300 – 500 MeV. So the heavy quark velocity is small:

$$v_Q \sim O\left(\frac{\Lambda_{QCD}}{m_Q}\right), \quad (3)$$

which is of the order of 10% for the B , and we can choose v_Q , or alternatively $1/m_Q$, as the expansion parameter for the NRQCD interactions. Now we have to determine the order in v of various correction terms. We can immediately write down the operators which appear with a tree level $1/m_Q$ coefficient: the non-relativistic kinetic energy operator

$$O_{\text{kin}} = -\frac{\vec{D}^2}{2m_Q} \quad (4)$$

and the magnetic interaction operator

$$O_{\text{mag}} = \frac{\vec{\sigma} \cdot \vec{B}}{2m_Q}. \quad (5)$$

To estimate the size of the heavy quark kinetic energy, we write

$$\frac{\vec{p}^2}{2m_Q} = \frac{(m_Q v)^2}{2m_Q} \sim \frac{\Lambda_{QCD}^2}{2m_Q}, \quad (6)$$

thus we expect O_{kin} to be suppressed with respect to D_t by a factor of $\Lambda_{QCD}/2m_Q$. For the magnetic operator we have

$$\vec{B} = \vec{\nabla} \times \vec{A}. \quad (7)$$

Since

$$A \sim p \sim O(\Lambda_{QCD}) \quad \text{and} \quad \nabla \sim p \sim O(\Lambda_{QCD}), \quad (8)$$

we estimate the magnetic operator to also be of order

$$O_{\text{mag}} \sim \frac{\Lambda_{QCD}^2}{2m_Q}. \quad (9)$$

The heavy quark formulation used in this calculation is described in more detail in section 2, where we also talk briefly about the implementation we use for the light quark and discuss the choice of our simulation parameters. In section 3

we show the operators from which our meson and baryon states are constructed. Details of our fitting procedure and the results are discussed in section 4. We also describe there how meson masses are extracted and give results for the B_d and the $B_s - B_d$ splitting. After that we turn to the $B^* - B$ (hyperfine) and $\Lambda_b - B$ splittings and compare simulation results with experimental values and expectations from HQET. Finally, we present preliminary results for P wave states. The conclusions are given in section 5.

2 Simulation details

The gauge fields used here are an ensemble of 35 quenched configurations at $\beta = 6.0$, generated by the UKQCD collaboration. The configurations are separated by 200 sweeps, each including 5 overrelaxation and 1 Cabibbo-Marinari heatbath sweep. By time reversing them, we obtain an additional set of 35 configurations which we treat in our analysis as statistically independent. We fixed the configurations to Coulomb gauge.

In this simulation the non-relativistic Lagrangian, which describes the b quark, is expanded through order $1/m_Q^0$ at tree level:

$$\mathcal{L} = Q^\dagger (D_t + H_0 + \delta H) Q, \quad (10)$$

where

$$H_0 = -\frac{\vec{D}^2}{2m_Q^0}, \quad \delta H = -\frac{c_B \vec{\sigma} \cdot \vec{B}}{2m_Q^0} \quad (11)$$

To get rid of large renormalizations of the link operator, we use tadpole improvement [14]:

$$U_\mu \rightarrow U_\mu/u_0, \quad u_0^4 = \langle \frac{1}{3} \text{Tr} U_{\text{Pla}} \rangle, \quad u_0 \simeq 0.878, \quad (12)$$

so we can use the tree level coefficient $c_B = 1$. The heavy quark propagator is computed using the following evolution equation [7]:

$$G_1 = \left(1 - \frac{aH_0}{2n}\right)^n U_4^\dagger \left(1 - \frac{aH_0}{2n}\right)^n \delta_{\vec{x},0}, \quad t = 1 \quad (13)$$

and on the following timeslices

$$G_{t+1} = \left(1 - \frac{aH_0}{2n}\right)^n U_4^\dagger \left(1 - \frac{aH_0}{2n}\right)^n (1 - a\delta H) G_t, \quad t > 1, \quad (14)$$

for the heavy quark masses $am_Q^0 = 1.71, 2.0, 2.5$ and 4.0 . The bare heavy quark mass corresponding to the b quark should be the same as the one tuned in Υ spectroscopy calculations with NRQCD. If the b quark mass is set to $am_b^0 = 1.71$, the simulated Υ mass agrees with the experimental value [7], using a lattice spacing of $2.4(1)$ GeV, obtained from the $1P - 1S$ and $2S - 1S$ splittings of the

Υ . However, due to the effect of quenching one obtains different lattice spacings from different physical quantities, or in other words, for different physical systems different scales are appropriate. From light hadron spectroscopy at the same value of β one gets lattice spacings closer to $a^{-1} \sim 2$ GeV. Probably, scales in heavy-light systems are closer to the ones in light hadrons. In this paper we use 2.05(10) GeV. The central value is taken from the APE collaboration who performed a spectrum calculation at the same value of β and the same type of light fermions (clover fermions with unity clover coefficient) and quote a value of $a^{-1} = 2.05(6)$ GeV from m_ρ [9]. We use a larger error for a^{-1} , to encompass other results from light spectroscopy (e.g. $a^{-1} = 2.11(11)$ from f_π in [9], $a^{-1} = 2.0 \pm \frac{3}{2}$ from m_ρ in [10].), as well as from the string tension [11] of $a^{-1} = 1.94(8)$ GeV at $\beta = 6.0$. Systematic errors in light hadron spectroscopy are still rather large and not well determined, so the uncertainty in a^{-1} may be underestimated. For $a^{-1} = 2.05$ GeV, $am_Q^0 = 2.0$ corresponds to the bare b quark mass used in the Υ simulations. The stability coefficient n has been set to 2 for all masses.

We also compute the heavy quark propagator in the zeroth order (static) approximation of the $1/m_Q^0$ expansion, where the Lagrangian is just given by the covariant time derivative:

$$\mathcal{L} = Q^\dagger D_t Q. \quad (15)$$

and the heavy quark propagator follows the evolution equation:

$$G_{t+1} - U_4^\dagger G_t = \delta_{(\vec{x},t),0}. \quad (16)$$

For the light quarks we use propagators generated by the UKQCD collaboration with a clover action [12]:

$$\begin{aligned} S_F = a^4 \sum_x \left[- \sum_\mu \frac{1}{a} \kappa \left(\bar{q}(x) (1 - \gamma_\mu) U_\mu(x) q(x + \mu) \right. \right. \\ \left. \left. + \bar{q}(x + \mu) (1 + \gamma_\mu) U_\mu^\dagger(x) q(x) \right) \right. \\ \left. + \frac{1}{a} \bar{q}(x) q(x) - i c a \kappa / 2 \sum_{\mu\nu} \bar{q}(x) \sigma_{\mu\nu} F_{\mu\nu} q(x) \right], \quad (17) \end{aligned}$$

with clover coefficient $c = 1$, i.e. *without* tadpole improvement. The quark fields are rotated at the source:

$$q(x) \rightarrow \left(1 - \frac{a}{2} \gamma \cdot D \right) q(x). \quad (18)$$

It has been shown [13] that matrix elements calculated with these quark fields are free of $O(a)$ errors at tree level.

We use light fermions at values of κ of 0.1440 and 0.1432, which bracket the strange quark mass. On the same set of configurations and light propagators the critical κ values has been determined to be 0.14556(6). The strange quark, whose mass is determined from m_K^2/m_ρ^2 , corresponds to $\kappa_s = 0.1437 \pm \frac{4}{5}$ [10].

3 Hadron operators

Our meson states are built up from various interpolating operators:

$$\sum_{\vec{x}_1, \vec{x}_2} Q^\dagger(\vec{x}_1) \Gamma^\dagger(\vec{x}_1 - \vec{x}_2) q(\vec{x}_2). \quad (19)$$

$\Gamma(\vec{x}_1 - \vec{x}_2)$ factorizes into a smearing function $\phi(r = |\vec{x}_1 - \vec{x}_2|)$ and an operator Ω which consists of a 4×2 matrix in spinor space and, for P states, a derivative acting on ϕ . We choose ϕ to be either a delta function or, to project onto the ground or an excited state, a hydrogen-like wave function. The smearing is applied on the heavy quark. In general the smearing function ϕ is different at the source (sc) and at the sink (sk), and we obtain meson propagators of the following form:

$$C(\vec{p} = 0, t) = \sum_{\vec{y}_1, \vec{y}_2} Tr \left[\gamma_5 (M^{-1})^\dagger(\vec{y}_2) \gamma_5 \Gamma^{(sk)\dagger}(\vec{y}_1 - \vec{y}_2) \tilde{G}_t(\vec{y}_1) \right]. \quad (20)$$

Here, M^{-1} is the light quark propagator and

$$\tilde{G}_t(\vec{y}) = \sum_{\vec{x}} G_t(\vec{y} - \vec{x}) \Gamma^{(sc)}(\vec{x}) \quad (21)$$

is the heavy quark propagator smeared at the source.

The continuum quantum numbers of the S and P states we implemented and the corresponding lattice operators Ω can be found in table 1. For the γ matrices we chose the Dirac basis using the representation

$$\gamma_0 = \begin{pmatrix} \mathbb{1} & 0 \\ 0 & -\mathbb{1} \end{pmatrix}, \quad \vec{\gamma} = \begin{pmatrix} 0 & -i\vec{\sigma} \\ i\vec{\sigma} & 0 \end{pmatrix}. \quad (22)$$

Note that in heavy-light systems C is not a good quantum number, and we expect mixing between the 3P_1 and the 1P_1 states.

For the Λ_b baryon we used the following interpolating operator:

$$O_\alpha = \epsilon_{abc} \sum_{\vec{x}_1} Q_\alpha^a(\vec{x}_1) \sum_{\vec{x}_2} (q^b)^T(\vec{x}_2) C \gamma_5 \gamma_0 q^c(\vec{x}_2) \phi(|\vec{x}_1 - \vec{x}_2|), \quad (23)$$

where $C = \gamma_0 \gamma_2$ is the charge conjugation matrix. The baryon correlators are smeared at the source and local at the sink.

4 Results

In the following we will use the notation C_{rs} for the correlation functions, where the index r denotes a delta function (L), ground state smearing function (1)

Meson ${}^{2S+1}L_J (J^P)$	Lattice Rep.	Ω
${}^1S_0 (0^-)$	A_1^-	$\begin{pmatrix} 0 \\ \mathbb{1} \end{pmatrix}$
${}^3S_1 (1^-)$	$T_{1(i)}^-$	$\begin{pmatrix} 0 \\ \sigma_i \end{pmatrix}$
${}^1P_1 (1^+)$	$T_{1(i)}^+$	$\begin{pmatrix} 0 \\ \Delta_i \end{pmatrix}$
${}^3P_0 (0^+)$	A_1^+	$\begin{pmatrix} 0 \\ \sum_j \Delta_j \sigma_j \end{pmatrix}$
${}^3P_1 (1^+)$	$T_{1(ij)}^+$	$\begin{pmatrix} 0 \\ \Delta_i \sigma_j - \Delta_j \sigma_i \end{pmatrix}$
${}^3P_2 (2^+)$	$E_{(ij)}^+$	$\begin{pmatrix} 0 \\ \Delta_i \sigma_i - \Delta_j \sigma_j \end{pmatrix}$
	$T_{2(ij)}^+$	$\begin{pmatrix} 0 \\ \Delta_i \sigma_j + \Delta_j \sigma_i \\ (i \neq j) \end{pmatrix}$

Table 1: Meson Operators. Δ_i denotes the symmetric lattice derivative. $\mathbb{1}$ stands for the 2×2 unit matrix.

or excited state smearing function (2) at the source. The index s denotes the smearing function at the sink.

From the original data we generated 100 bootstrap ensembles, each containing the original number of samples, and fitted to each of them separately. The fit results and errors are obtained from averaging over the number of bootstrap samples. This procedure also enables us to take correlations between data with different κ and m_Q^0 values from the same configuration into account. Given the relatively low statistics, we are sometimes forced to discard eigenvalues in our SVD inversion of the covariance matrix. This is done using a cutoff λ on the ratio between the smallest and the largest eigenvalue.

4.1 Ground state energy

To extract the bare ground state energy, E_{sim} , and amplitudes we fitted the correlators C_{1L} and C_{11} simultaneously to a single exponential. The signal is good up to large times and we fit out until $t_{\text{max}} = 25$. The plateau of the correlation functions at $\kappa = 0.1432$ is reached at $t_{\text{min}} = 5$, but at $\kappa = 0.1440$ there is a slight decrease in the ground state energy and especially the amplitudes until t_{min} is moved out to 9. Moving t_{min} further out does not change the results any more. An example for the dependence of the ground state energy on the fit interval at the different κ values is shown in table 2, together with the quality of fit parameter Q .

With our limited statistics, our bootstrap procedure generates certain ensembles on which multi-exponential fits fail, but with the original ensemble of correlation functions we can do a simultaneous fit of C_{1L} and C_{2L} to 2 exponentials. This gives a value for the ground state energy which tends to be a little higher, but in general still compatible within one standard deviation with the results fitted with just one exponential. Results of double exponential fits for $am_Q^0 = 4.0$ are shown in table 3. The single exponential fits give higher Q values and better looking effective mass plots, so we use them to extract the meson ground state energies. We can also make a rough estimate of the energy of the first excited state. Its error bars are too large to extract a dependence on the heavy or the light quark masses. From the results in table 3 and fit results at other heavy quark masses we take the value of $E_{\text{sim}}(2S) = 0.8(1)$ as a reasonable estimate. For a more reliable calculation of the excited state energy one would have to do three exponential fits to C_{1L} and C_{2L} , but, given our low statistics, errors on these fits are very large.

We extract meson energies from fits in the range $t_{\text{min}}/t_{\text{max}} = 9/25$ for both κ values. The systematic error due to the variation of the fit interval and the difference between the single and double exponential fits is smaller than the fit error at this fit range. Effective mass plots for C_{1L} and C_{11} are shown in figure 1. Results for the pseudoscalar, vector and spin-averaged ground state energy $\bar{E} = (3E_{\text{sim}}(^3S_1) + E_{\text{sim}}(^1S_0))/4$ for all heavy and light quark mass values are shown

	$\kappa = 0.1432$		$\kappa = 0.1440$	
t_{min}/t_{max}	$aE_{sim}(1S)$	Q	$aE_{sim}(1S)$	Q
5/25	0.516(6)	0.3	0.497(6)	0.2
6/25	0.515(7)	0.4	0.495(7)	0.2
7/25	0.514(6)	0.4	0.493(8)	0.2
8/25	0.514(7)	0.4	0.491(7)	0.3
9/25	0.513(7)	0.4	0.491(8)	0.3
10/25	0.511(5)	0.4	0.489(7)	0.3

Table 2: Results of single exponential fits to the ground state correlation functions C_{11} and C_{1L} at $am_Q^0 = 4.0$. For $\kappa = 0.1432$, $\lambda = 0.03$, for $\kappa = 0.1440$, $\lambda = 0.02$.

	$\kappa = 0.1432$			$\kappa = 0.1440$		
t_{min}/t_{max}	$aE_{sim}(1S)$	$aE_{sim}(2S)$	Q	$aE_{sim}(1S)$	$aE_{sim}(2S)$	Q
4/24	0.513(4)	0.81(4)	0.07	0.495(6)	0.79(5)	0.09
5/25	0.518(5)	0.77(6)	0.17	0.497(7)	0.71(6)	0.19
6/25	0.516(5)	0.79(8)	0.15	0.495(9)	0.71(9)	0.15
7/25	0.519(3)	0.94(34)	0.09	0.502(5)	0.92(25)	0.08
8/25	0.520(7)	0.91(18)	0.07	0.498(3)	0.92(43)	0.11
9/25	0.517(7)	0.90(18)	0.06	0.501(5)	0.88(25)	0.09
10/25	0.517(6)	0.88(16)	0.03	0.501(2)	0.86(8)	0.07

Table 3: Results of double exponential fits to the correlation functions C_{1L} and C_{2L} for $am_Q^0 = 4.0$, $\lambda = 10^{-5}$.

in table 4, the chiral extrapolation and interpolation to the strange light quark mass in table 5.

The dependence of the bare spin-averaged ground state energy on the bare heavy quark mass is illustrated in figure 2. This quantity is spin-independent and thus useful to estimate the correction due to the kinetic operator O_{kin} . Correlated fits of the simulation results to linear functions give a slope of $-0.02(2)$ in lattice units for $\kappa = 0.1440$ and for $\kappa = 0.1432$, $-0.02(1)$. In both cases, the extrapolation to the static limit is compatible with the static simulation results. We note that in the tadpole improved case, O_{kin} is not a positive definite operator. A more physical quantity than E_{sim} is the binding energy, $E_{bind} = E_{sim} - E_0$, where E_0 is the shift in the zero of energy for NRQCD or the static theory, respectively (perturbative values from [15] listed in table 6). This quantity rises slightly as a function of $1/m_Q^0$, but there are significant perturbative uncertainties. For a more detailed discussion see [16].

		$\kappa = 0.1432$		$\kappa = 0.1440$	
${}^{3S+1}L_J$	am_Q^0	aE_{sim}	Q	aE_{sim}	Q
1S_0	1.71	0.501(9)	0.3	0.480(7)	0.4
	2.0	0.506(6)	0.4	0.483(7)	0.4
	2.5	0.511(5)	0.4	0.487(7)	0.4
	4.0	0.513(7)	0.3	0.491(8)	0.3
	∞	0.524(6)	0.2	0.508(7)	0.2
3S_1	1.71	0.521(6)	0.3	0.502(7)	0.4
	2.0	0.523(5)	0.3	0.503(6)	0.3
	2.5	0.524(6)	0.3	0.504(6)	0.3
	4.0	0.527(6)	0.3	0.507(8)	0.2
spin avg.	1.71	0.516(6)	0.3	0.497(7)	
	2.0	0.518(5)	0.3	0.498(7)	
	2.5	0.521(6)	0.3	0.499(7)	
	4.0	0.524(6)	0.3	0.503(7)	

Table 4: Fit results for the bare ground state energy for the pseudoscalar and the vector meson and the spin-averaged energy for both κ values.

		$m_q = 0$	$m_q = m_{\text{strange}}$
${}^{3S+1}L_J$	am_Q^0	aE_{sim}	aE_{sim}
1S_0	1.71	0.437(19)	0.489(6)
	2.0	0.437(11)	0.491(6)
	2.5	0.439(12)	0.496(7)
	4.0	0.446(15)	0.499(6)
	∞	0.461(15)	0.511(6)
3S_1	1.71	0.464(15)	0.509(6)
	2.0	0.463(12)	0.510(6)
	2.5	0.464(9)	0.512(6)
	4.0	0.478(12)	0.515(6)
spin avg.	1.71	0.457(14)	0.504(6)
	2.0	0.456(12)	0.505(6)
	2.5	0.457(9)	0.508(6)
	4.0	0.462(13)	0.511(6)

Table 5: Bare ground state energy, extrapolated to a vanishing (left) and the strange (right) light quark mass.

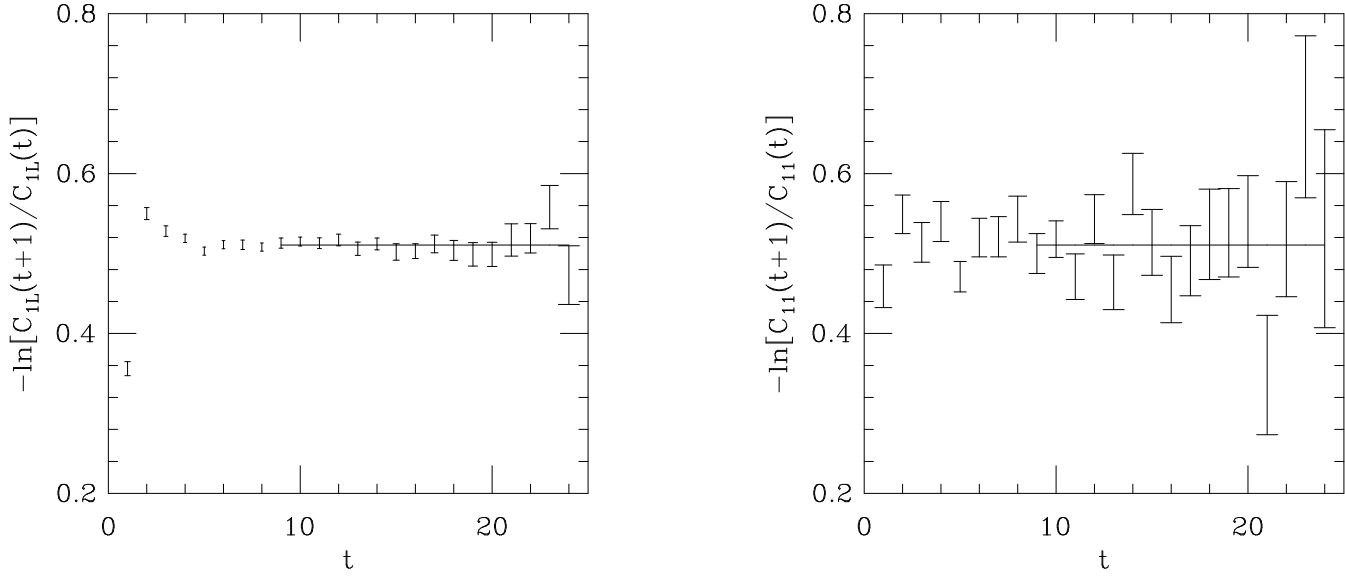


Figure 1: Effective masses of C_{1L} (left) and C_{11} (right) correlation functions at $am_Q^0 = 2.5$ and $\kappa = 0.1432$.

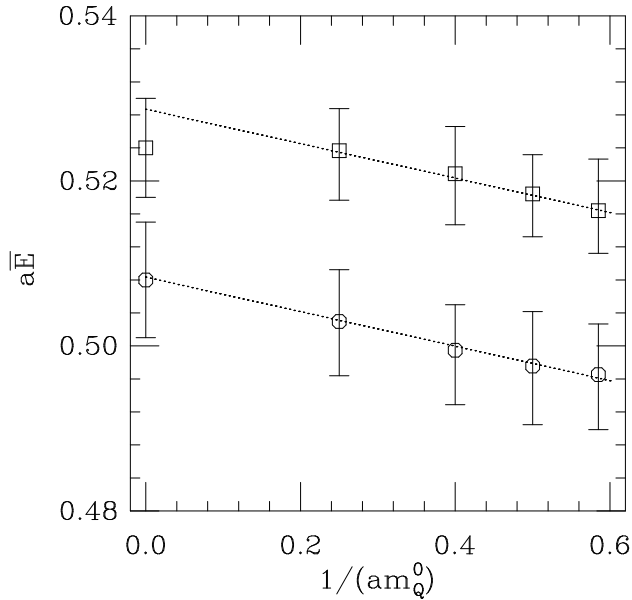


Figure 2: Bare spin-averaged ground state energy as a function of the inverse bare heavy quark mass am_Q^0 . Squares denote $\kappa = 0.1432$ and circles $\kappa = 0.1440$. The lines represent correlated fits of the NRQCD results to a linear function.

am_Q^0	n	aE_0	$a\Delta$	aM_P			$M_{P_d}[\text{GeV}]$
				$\kappa = 0.1432$	$\kappa = 0.1440$	$m_q = 0$	
1.71	2	0.32(6)	1.73(13)	2.23	2.21	2.17	4.5(5)
2.0	2	0.30(6)	2.02(12)	2.53	2.50	2.46	5.1(5)
2.5	2	0.29(6)	2.48(9)	2.99	2.97	2.92	6.0(5)
4.0	2		4.07(5)	4.58	4.56	4.52	9.3(6)

Table 6: Energy shifts used in our calculation and pseudoscalar meson masses calculated with these shifts. The last column contains meson masses for $m_q \rightarrow 0$ in physical units, using a lattice spacing of $a^{-1} = 2.05(10)$ GeV. Errors on aM_P are dominated by the perturbative error in Δ , errors on the physical masses by perturbation theory and the uncertainty in the lattice spacing.

4.2 Meson masses

We calculate the meson mass using the relation

$$M_B = \Delta + E_{\text{sim}}. \quad (24)$$

The energy shift Δ can be determined in perturbation theory. It consists of the renormalized heavy quark mass and a shift in the zero of energy:

$$\Delta = Z_m m_Q^0 - E_0. \quad (25)$$

The quantities Z_m and E_0 are calculated at $O(\alpha)$:

$$aE_0 = A\alpha_V(q_A^*), \quad Z_m = 1 + B\alpha_V(q_B^*), \quad (26)$$

where we take for α_V the two loop expression for the running coupling constant in the Lepage-Mackenzie scheme. The one loop terms A and B and the appropriate momentum scales q_A^* and q_B^* were calculated by C. Morningstar [15]. The shifts used in our calculation are shown in table 6, together with results for the meson masses in lattice and physical units. E_0 values are perturbative, shifts are perturbative except in the last row. At $m_Q^0 = 4.0$, a non-perturbative energy shift calculated from the Υ has been used, to avoid defects in the scale q_B^* in the heavy quark mass renormalization, occurring at heavy quark masses around $am_Q^0 = 5$. It is possible to calculate the meson mass non-perturbatively from the meson dispersion relation [17]. The non-relativistic dispersion relation reads in lowest order:

$$E(\vec{p}) = E(\vec{p} = \vec{0}) + \frac{\vec{p}^2}{2M_B}. \quad (27)$$

Note that $E(\vec{p} = 0)$ is, by definition, E_{sim} . We calculate the ‘kinetic’ meson mass M_B from the energy splitting between mesons of momentum $|\vec{p}| = 2\pi/L_s$ and $|\vec{p}| = 0$, where L_s is the spatial lattice extent.

am_Q^0	$\kappa = 0.1432$			$\kappa = 0.1440$		
	$a\Delta E$	Q	aM_P	$a\Delta E$	Q	aM_P
1.71	0.030(7)	0.5	2.6(6)	0.034(5)	0.5	2.3(3)
2.0	0.030(12)	0.5	2.6(1.0)	0.030(5)	0.5	2.6(4)
2.5	0.024(8)	0.5	3.2(1.1)	0.026(5)	0.5	3.0(6)
4.0	0.018(8)	0.4	4.3(1.9)	0.018(5)	0.5	4.3(1.2)

Table 7: Splitting between correlation functions with $|\vec{p}| = 2\pi/L_s$ and $|\vec{p}| = 0$ and meson masses derived from it.

In our analysis of the energy splittings between the finite and zero momentum correlation functions we make use of the fact that correlation functions of different states on the same configuration are highly correlated. We generate 100 bootstrap measurements of the jackknifed ratio R of the correlation functions of the two states and fit these to a single exponential:

$$R \sim Ae^{-\Delta Et}, \quad (28)$$

where ΔE is the energy splitting.

As shown in table 7, the masses obtained with this method have much larger errors, but are compatible with the masses calculated using perturbation theory.

4.3 Mass splittings

4.3.1 $B_s - B_d$ splitting

am_Q^0	$a\Delta E$
1.71	0.047(11)
2.0	0.049(8)
2.5	0.050(5)
4.0	0.049(7)
∞	0.051(13)

Table 8: Spin-averaged $B_s - B_d$ splitting.

Results for the spin-averaged $B_s - B_d$ splitting are listed in table 8. As expected from HQET, this splitting is fairly independent of the heavy quark mass. Figure 3 shows the splitting as a function of the inverse spin-averaged meson mass with a correlated fit to a constant. The fitted value for this constant is 0.049(5), with a χ^2 per degree of freedom of 0.03. Converted into physical

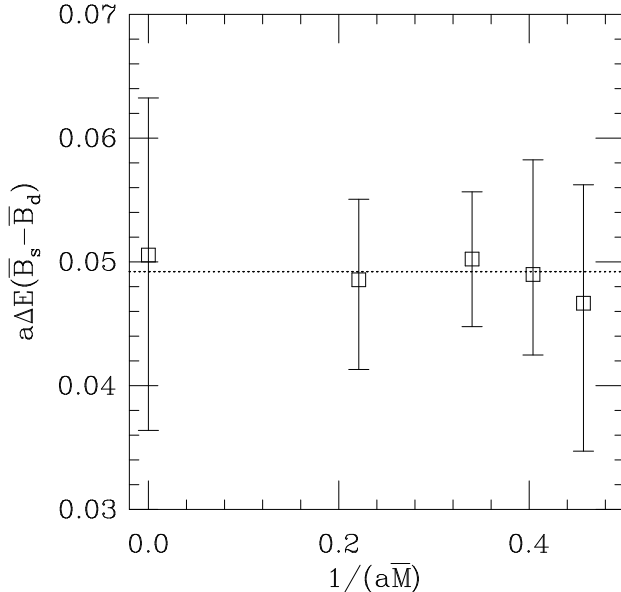


Figure 3: Spin-averaged energy splitting between B_s and B_d in lattice units plotted against the inverse spin-averaged meson mass. The dotted line denotes a correlated fit of the simulation results to a constant.

	$\kappa = 0.1432$		$\kappa = 0.1440$	
am_Q^0	$a\Delta E$	Q	$a\Delta E$	Q
1.71	0.0201(17)	0.43	0.0200(24)	0.42
2.0	0.0180(14)	0.51	0.0180(20)	0.47
2.5	0.0151(12)	0.43	0.0150(17)	0.37
4.0	0.0103(10)	0.28	0.0102(14)	0.22

Table 9: Fit results for the $B^* - B$ splitting in lattice units, $\lambda = 5 \times 10^{-2}$.

units this is 100(14) MeV, which is in good agreement with the experimental value of 97(6) MeV. This also means that κ_s as determined from the K mass is appropriate to the B_s system.

4.3.2 Hyperfine splitting

For the hyperfine splitting we use the ratio fit method as described in section 4.2 for the splitting between finite and zero momentum correlation functions. The fit interval is chosen to be $t_{min}/t_{max} = 9/25$. An effective mass plot is shown in figure 4. The fit results are given in table 9. There is no visible dependence on the light quark mass. This also holds for the experimental results, which are 46.0(6) MeV for the $B^* - B$ splitting and 47.0(2.6) MeV for the $B_s^* - B_s$ splitting.

We find our simulation results for the splitting to be approximately propor-

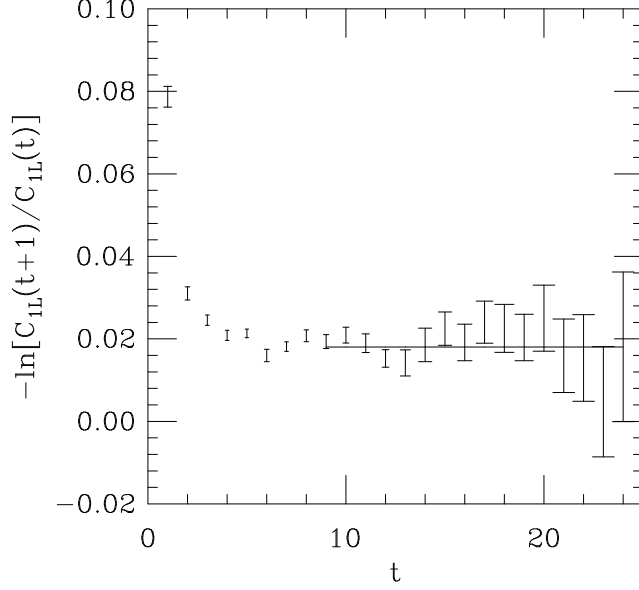


Figure 4: Effective mass of the ratio of the correlation functions of the B^* and the B at $am_Q^0 = 2.0$, $\kappa = 0.1432$. The solid line denotes the fit.

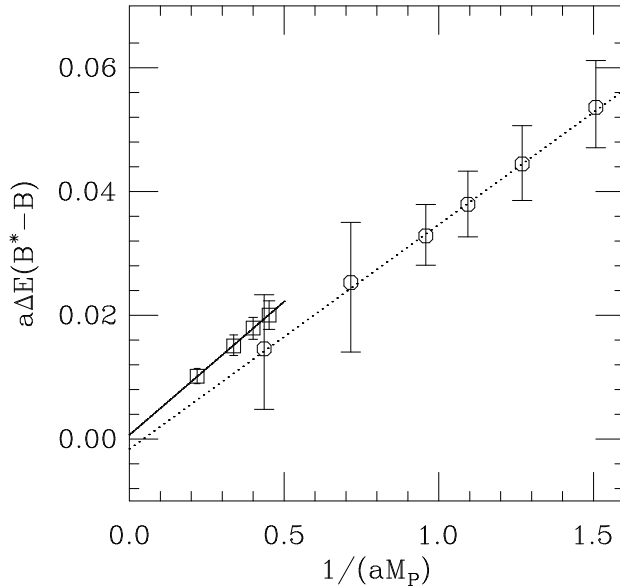


Figure 5: $B^* - B$ splitting at $\kappa = 0.1440$ plotted against the inverse pseudoscalar meson mass. Squares denote NRQCD results and circles, UKQCD results using the clover formulation for the heavy quark, plotted against the inverse dynamical meson mass [19]. The dotted lines show correlated fits of the data to linear functions. Errors in the meson mass are not shown for clarity.

tional to the heavy meson mass:

$$\Delta E \propto 1/M_P. \quad (29)$$

This is illustrated in figure 5. Using a correlated fit to the results at $\kappa = 0.1440$ it is found that the splitting extrapolates to $a\Delta E = 0.001(2)$ as $M_P \rightarrow \infty$. This is consistent with zero, as it should be. The fit result for the slope is $0.043(6)$. From a fit to the simulation results at $\kappa = 0.1432$ one obtains very similar values for the static extrapolation and the slope. Converting the value corresponding to the physical B mass into physical units, we obtain 36 MeV. This is relatively close to the experimental value, but slightly low. This might be an effect of quenching, which is expected to decrease the wave function at the origin and thus the hyperfine splitting. The error is 5 MeV if uncertainties in the lattice spacing are not taken into account; if they are included one obtains an error of 9 MeV. Note that errors in a^{-1} effectively appear squared in the hyperfine splitting, as they affect both the value of the splitting and the meson mass at which the splitting is taken. Previous studies [18] by UKQCD using a relativistic quark action for the heavy quark have given much lower results, which are incompatible with experiment, when plotted against the ‘static’ meson mass. As we show in figure 5, their results, using the same ensemble of gauge field configurations and light propagators and clover fermions without tadpole improvement for the heavy quark, are compatible with ours when plotted against the kinetic mass [19]. However there is a systematic uncertainty in the determination of the kinetic mass for clover fermions of about 20 % around the B , as well as statistical errors that are larger than 30 % in the region of the B .

4.3.3 $\Lambda_b - \overline{B}$ and $\Lambda_b - B$ splittings

An example for the effective mass of the correlation function of the Λ_b baryon is shown in figure 6. The bare binding energy of the Λ_b is determined from a fit of the correlation function to a single exponential. The interval is chosen to be $t_{min}/t_{max} = 7/13$ for $\kappa = 0.1440$ and $t_{min}/t_{max} = 7/16$ for $\kappa = 0.1432$. The results are given in table 10. The splitting between the Λ_b and the meson is determined by calculating the bootstrapped difference between the ground state energies of both states. On our ensemble there are large error bars on the baryon energy. From HQET we expect that the splitting between the Λ_b and the spin average of the B and the B^* , \overline{B} , should be fairly independent of the heavy quark mass. In the Λ_b the b quark couples to a spin zero system of light quarks. In the B and the B^* , b couples to a light quark of spin 1/2, giving a hyperfine splitting which is a $1/m_Q$ effect. This expectation is fulfilled well for our results, as is shown in figure 7, and is borne out by experiment, $\Delta E(\Lambda_b - \overline{B})$ being 330(50) MeV and $\Delta E(\Lambda_c - \overline{D})$ being 313(1) MeV. Performing a correlated fit of the splittings at all our heavy quark masses to a constant C , one obtains $C = 0.20(3)$, with a χ^2 per degree of freedom of 0.01. The mass independence of this splitting

am_Q^0	$\kappa = 0.1432$		$\kappa = 0.1440$	
	aE_{sim}	Q	aE_{sim}	Q
1.71	0.82(1)	0.25	0.76(2)	0.41
2.0	0.82(1)	0.31	0.76(2)	0.43
2.5	0.82(2)	0.31	0.77(2)	0.47
4.0	0.82(2)	0.34	0.77(2)	0.40

Table 10: Fit results for the Λ_b ground state energy in lattice units.

am_Q^0	$a\Delta E(\Lambda_b - B)$	$a\Delta E(\Lambda_b - \overline{B})$
1.71	0.21(7)	0.19(6)
2.0	0.22(4)	0.20(5)
2.5	0.22(4)	0.20(4)
4.0	0.21(4)	0.20(5)

Table 11: Chirally extrapolated splitting between the Λ_b and the B and between the Λ_b and the spin average between the B and B^* , in lattice units.

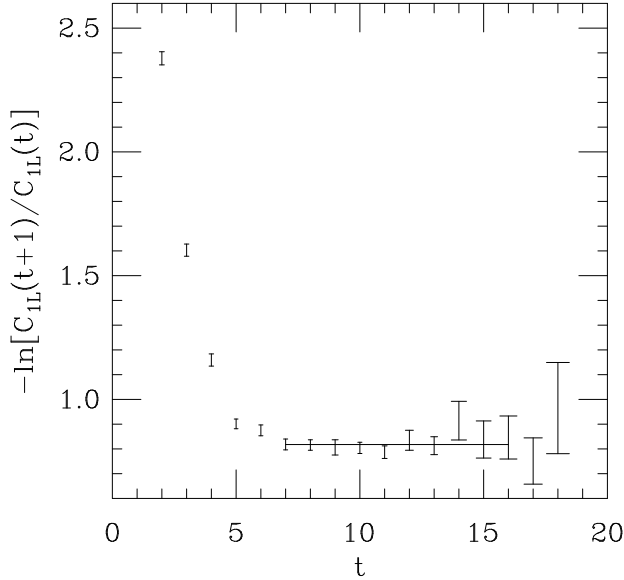


Figure 6: Effective mass of the Λ_b correlation function at $am_Q^0 = 2.0$, $\kappa = 0.1432$. The solid line denotes the fit.

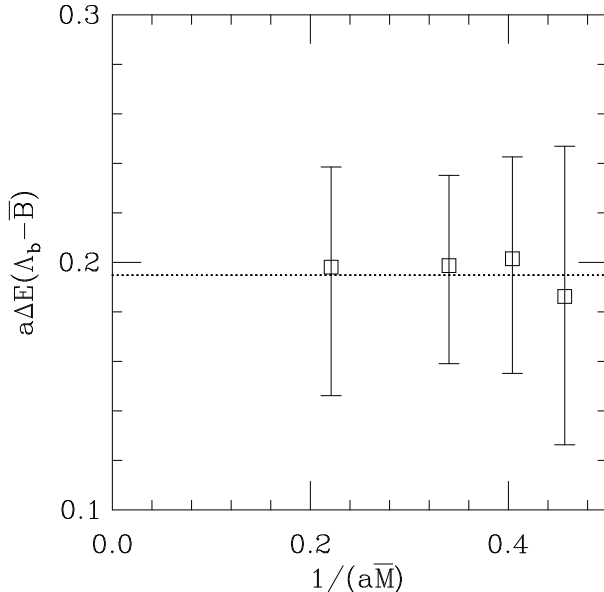


Figure 7: The chirally extrapolated splitting between the Λ_b and the spin-average of the B and B^* , plotted against the inverse spin-averaged meson mass. The dotted line shows a correlated fit of the data to a constant.

makes it a good quantity to calculate and we could actually use it to extract a^{-1} . Using the experimental value for the splitting at the B , we obtain $a^{-1} = 1.7(2)$ GeV. Converting the constant C into physical units, using a lattice spacing of $a^{-1} = 2.05(10)$ GeV, one obtains $0.41(9)$ GeV. Our central value is slightly higher than the experimental result, albeit with large errors. It is possible that the Λ_b suffers finite volume effects on these lattices.

C is also our prediction for the static $\Lambda_b - B$ splitting, which is in good agreement with the static result of the UKQCD collaboration at $\beta = 6.2$ of $0.42 \pm_{9}^{10}(stat) \pm_{3}^{3}(syst)$ GeV [5]. Our correlation functions for the static Λ_b are rather noisy at this level of statistics and it is problematic to extract baryon energies from them.

Other groups extract results for the $\Lambda_b - B$ splitting. This is expected to be more dependent on the heavy quark mass. Experimentally, one has $\Delta E(\Lambda_b - B) = 0.36(5)$ GeV and $\Delta E(\Lambda_c - D) = 0.416(1)$ GeV. We work at the b quark mass and can extract a splitting of $0.43(10)$ GeV. In fact there is no noticeable mass dependence in our $\Lambda_b - B$ splitting in table 11, but our error bars are larger than the hyperfine splitting, so at our level of statistics we could not clearly detect it. However, without chiral extrapolation the mass dependence is somewhat more obvious. Other groups have used a relativistic quark action and extrapolated from moderate quark masses to the b (for a compilation of results see [21]). This is dangerous, particularly if such an extrapolation has been shown to give an incorrect hyperfine splitting. We believe that there could be significant systematic errors attached to this procedure.

4.3.4 $P - S$ splitting

The observation of orbitally excited mesons, generically called B^{**} states, has been reported recently by DELPHI and OPAL [22, 23]. They study decay modes to $B\pi$ and $B^*\pi$ and are not able to clearly separate the expected 0^+ , 1^+ , $1^{+'}$ and 2^+ resonances, the first two expected to be rather broad ($j_q = 1/2$) and the latter two, narrow ($j_q = 3/2$). A mass of 5.73(25) GeV is quoted for the cross-section weighted mean mass of B^{**} states by DELPHI. This gives some ambiguity when we wish to compare lattice calculations with experiment. The ideal quantity to calculate is the spin-averaged splitting, $\overline{B^{**}} - \overline{B}$. The experiments above give a $B^{**} - \overline{B}$ splitting of 419(25) MeV without spin-averaging. Thus individual B^{**} states, and hence the spin-average may differ from this value by the splittings between P states, and it is unknown how individual states contribute to the experimental number. A splitting of around 50 MeV between the $j_q = 3/2$ and the $j_q = 1/2$ states has been suggested [24]. For the case of charm the two narrow 2^+ and $1^{+'}$ states have been clearly seen and yield a $D(1^{+'}) - \overline{D}$ splitting of 450(3) MeV. This is very similar to the number above and indicates that the heavy quark mass dependence of the $P - \overline{S}$ splitting isn't large and will only be visible once the separation of P states is clear.

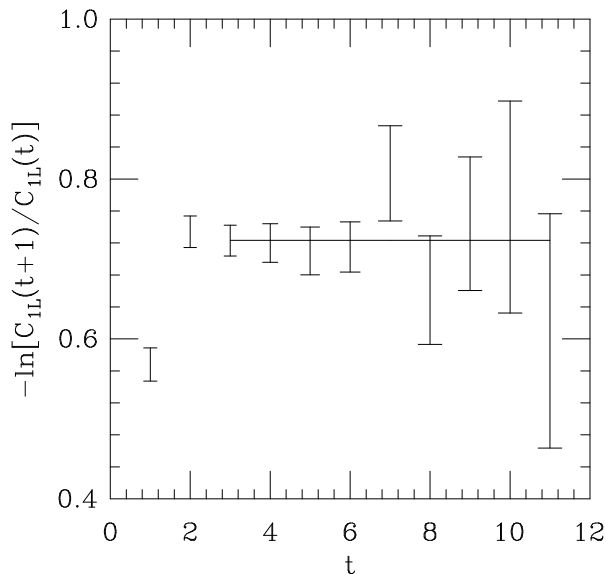


Figure 8: Effective mass of the 1P_1 correlation function, $am_Q^0 = 2.0$, $\kappa = 0.1432$. The solid line denotes the fit.

For our P state correlation functions, we are only able to extract a good signal from the 1P_1 . The 3P_0 , 3P_1 and 3P_2 are rather noisier and give, where visible, a very similar effective mass to that of the 1P_1 . We have not considered the $^1P_1/{}^3P_1$ cross-correlations, so it is not clear whether the mass we are extracting

	$\kappa = 0.1432$		$\kappa = 0.1440$	
am_Q^0	E_{sim}	Q	E_{sim}	Q
1.71	0.70(4)	0.39	0.72(4)	0.39
2.0	0.72(1)	0.27	0.72(1)	0.25
2.5	0.71(1)	0.26	0.71(1)	0.23
4.0	0.71(1)	0.32	0.71(2)	0.38

Table 12: Fit results for the 1P_1 states.

am_Q^0	$a\Delta E$
1.71	0.27(4)
2.0	0.27(2)
2.5	0.25(2)
4.0	0.25(2)

Table 13: $^1P_1 - \bar{S}$ splitting.

from the 1P_1 is that of the physical 1^+ or the $1^{+'}$ or some average. This theoretical uncertainty, which can be improved with a higher statistics calculation and taking the cross-correlations into consideration [26], is similar to the current experimental uncertainty described above.

For the heavy quark masses 2.0, 2.5 and 4.0, a fit interval of $t_{\text{min}}/t_{\text{max}} = 3/11$ was chosen for our 1P_1 correlation functions. An example for an effective mass plot is shown in figure 8. In the run with $am_Q^0 = 1.71$ the smearing functions for the P states were less optimized, so there a fit interval of $t_{\text{min}}/t_{\text{max}} = 8/12$ was used. The results for the 1P_1 seem to be independent of the light quark mass, so we choose to determine the $S - P$ splitting by calculating the bootstrapped difference between the 1P_1 simulation energy at $\kappa = 0.1432$ and the chirally extrapolated spin-averaged S state simulation energy.

In figure 9 we show the $S - P$ splitting plotted against the inverse spin-averaged meson mass. The dependence on heavy quark mass is clearly small, as expected. A correlated fit to a linear function gives an extrapolation to the static value of 0.22(5) in lattice units and a slope of 0.1(1), compatible with zero. Taking our result at $am_Q^0 = 2.0$, which is approximately at the B , and $a^{-1} = 2.05(10)$ GeV gives a splitting of 0.55(4) GeV. This is rather higher than the experimental value above but not inconsistent given the systematic errors arising from the uncertainty (both theoretical and experimental) over which B^{**} state we are considering. If we use the experimental result to derive a lattice spacing, we obtain the rather low value 1.6(2) GeV, in fact in agreement with our result

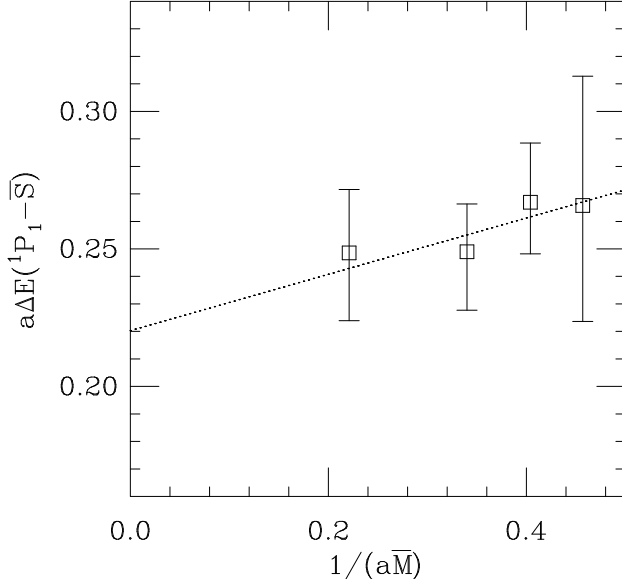


Figure 9: The $^1P_1 - \bar{S}$ splitting plotted against the inverse spin-averaged meson mass. The dotted line corresponds to a correlated fit of the lattice results to a linear function.

from $\Lambda_b - \bar{B}$. Previous results in the static approximation [25] give a splitting of around 0.4 GeV for the $B(1^+) - \bar{B}$ splitting. There is some indication in our results that the static value might be slightly lower than that at the b mass, but we have not attempted to calculate this splitting in the static approximation.

5 Conclusions

We present the first comprehensive lattice study of the heavy-light spectrum at meson masses in the region of the B in the quenched approximation, using NRQCD and static heavy quarks. The light fermion action has been improved through $O(a)$ at tree level, and the NRQCD action has been tadpole improved. Work is in progress using tadpole improved light fermions with higher statistics [27].

Our work has shown that with our method it is feasible to simulate heavy-light hadrons with a b quark directly on the lattice. Results for meson masses, the hyperfine splitting, $B_s - B_d$ splitting, P wave states and heavy-light baryons have been obtained that are in reasonable agreement with experiment. A comparison between the lattice results and experimental values is shown in figure 10. Note that in figure 10 we have fixed the B mass to its experimental value and plotted splittings in physical units. This study on quenched configurations has been performed in parallel with an investigation with 2 flavours of dynamical quarks [16, 20], which enables us in principle to estimate the dependence of the

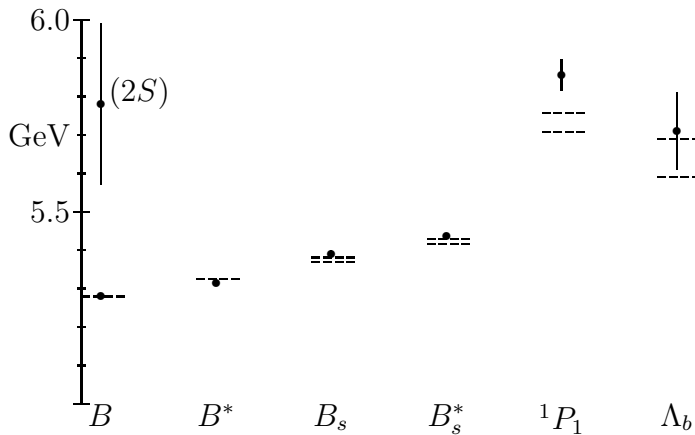


Figure 10: The B spectrum. Filled circles denote our results, where error bars do not take uncertainties in a^{-1} and the perturbative energy shifts into account. The dashed lines denote the upper and lower bounds on the experimental data. The mass of the B has been shifted upwards to match the physical value.

results on the number of flavours.

Acknowledgements

We are grateful to the UKQCD collaboration for allowing us to use their gauge configurations and light propagators. We would like to thank C. Morningstar and G. P. Lepage for useful discussions. This work was supported by SHEFC, PPARC and the U.S. DOE. We acknowledge support by the NATO under grant CRG 941259 and the EU under contract CHRX-CT92-0051. We thank the Edinburgh Parallel Computing Centre for providing computer time on their CM-200.

References

- [1] For a review see for example: J. L. Rosner, in *B Decays*, ed. S. Stone, World Scientific (1994) 470.
- [2] M. Voloshin and M. Shifman, *Sov. J. Nucl. Phys.* **45** (1987) 292; *Sov. J. Nucl. Phys.* **47** (1998) 511;
H. Politzer and M. Wise, *Phys. Lett.* **B206** (1989) 681; *Phys. Lett.* **B 208**(1989) 504.
N. Isgur and B. Wise, *Phys. Lett.* **B 232** (1989) 113; *Phys. Lett.* **B237** (1990) 527;
E. Eichten and B. Hill, *Phys. Lett.* **B234** (1990) 511;

- B. Grinstein, Nucl. Phys. **B339** (1990) 253;
H. Georgi, Phys. Lett. **B240** (1990) 447.
- [3] P. B. Mackenzie, Nucl. Phys. **B** (Proc. Suppl.) **30** (1993) 35.
- [4] S. Collins, R. Edwards, U. Heller and J. Sloan, poster presented by S. Collins and J. Sloan at the *International Symposium on Lattice Field Theory, Melbourne, Australia, 11–15 July 1995*, to appear in Nucl. Phys. **B** (Proc. Suppl.).
- [5] UKQCD Collaboration, Preprint Edinburgh 95/550, Southampton SHEP 95-20 and Swansea SWAT/78, hep-lat/95-8030.
- [6] G. P. Lepage, L. Magnea, C. Nakhleh, U. Magnea and K. Hornbostel, Phys. Rev. **D46** (1992) 4052.
- [7] C. T. H. Davies, K. Hornbostel, A. Langnau, G. P. Lepage, A. Lidsey, J. Shigemitsu and J. Sloan, Phys. Rev. **D50** (1994) 6963.
- [8] C. T. H. Davies *et al.*, to appear in Phys. Rev. **D52** (1995).
- [9] C. R. Allton *et al.*, APE collaboration, Nucl. Phys. **B413** (1994) 461.
- [10] UKQCD Collaboration, Phys. Rev. **D49** (1994) 1594.
- [11] G. Bali and K. Schilling, Phys. Rev. **D48** (1994) 2636.
- [12] B. Sheikholeslami and R. Wohlert, Nuclear Physics **B259** (1985) 572.
- [13] G. Heatlie, C. T. Sachrajda, G. Martinelli, C. Pittori and G. C. Rossi, Nucl. Phys. **B352** (1991) 266.
- [14] G. P. Lepage and P. B. Mackenzie, Phys. Rev. **D48** (1993) 2250.
- [15] C. J. Morningstar, Phys. Rev. **D48** (1993) 2265 and private communication.
- [16] *B Spectroscopy From NRQCD with Dynamical Fermions*, S. Collins, U. M. Heller, J. H. Sloan, J. Shigemitsu, C. T. H. Davies and A. Ali Khan, in preparation.
- [17] C. T. H. Davies, K. Hornbostel, A. Langnau, G. P. Lepage, A. J. Lidsey, C. J. Morningstar, J. Shigemitsu and J. Sloan, Phys. Rev. Lett. **73** (1994) 2657.
- [18] UKQCD Collaboration, presented by D. G. Richards, Nucl. Phys. **B** (Proc. Suppl.) **30** (1993) 389.
- [19] S. Collins, PhD thesis, unpublished results.

- [20] S. Collins, A. Ali Khan, C. T. H. Davies, J. Shigemitsu, U. M. Heller and J. Sloan, Nucl. Phys. **B** (Proc Suppl.) **42** (1995) 394.
- [21] *Heavy Baryon Spectroscopy on the Lattice*, UKQCD Collaboration, Preprint Edinburgh 95/555, Marseille CPT-95/PE.3244, Southampton SHEP-95/31, to appear.
- [22] DELPHI Collaboration, Phys. Lett. **B345** (1995) 598.
- [23] OPAL Collaboration, Z. Physik **C66** (1995) 19.
- [24] J. L. Rosner, Comm. Nucl. Part. Phys. **16** (1986) 109.
- [25] A. Duncan *et al.*, presented by E. Eichten and B. Hill, Nucl. Phys. **B** (Proc. Suppl.) **30** (1993) 433.
- [26] For an example of this procedure see *B_c Spectroscopy from Lattice QCD*, C. T. H. Davies *et al.*, in preparation.
- [27] A. Ali Khan *et al.*, in progress.